Liquid Crystals
Publication details, including instructions for authors and subscription information:
http://www.informaworld.com/smpp/title~content=t713926090

Novel mesophases in fluorine substituted banana-shaped mesogens

J. P. Bedel[a]; J. C. Rouillon[a]; J. P. Marcerou[a]; M. Laguerre[b]; H. T. Nguyen[a]; M. F. Achard[a]
[a] Centre de Recherche Paul Pascal, Université Bordeaux I, Av. A. Schweitzer, 33600 Pessac, France France, [b] Institut Européen de Chimie et Biologie, Ecole Polytechnique-Universite Bordeaux I-Universite Bordeaux II, Avenue Pey-Berland, 33402 Talence, France,

Online publication date: 06 August 2010

To cite this Article Bedel, J. P. , Rouillon, J. C. , Marcerou, J. P. , Laguerre, M. , Nguyen, H. T. and Achard, M. F.(2000) 'Novel mesophases in fluorine substituted banana-shaped mesogens', Liquid Crystals, 27: 11, 1411 — 1421
To link to this Article: DOI: 10.1080/026782900750018555
URL: http://dx.doi.org/10.1080/026782900750018555

LIQUID CRYSTALS, 2000, VOL. 27, NO. 11, 1411–1421

Novel mesophases in fluorine substituted banana-shaped mesogens

J. P. BEDEL, J. C. ROUILLON, J. P. MARCEROU, M. LAGUERRE†,
H. T. NGUYEN and M. F. ACHARD*

Centre de Recherche Paul Pascal, Université Bordeaux I, Av. A. Schweitzer,
33600 Pessac, France
† Institut Européen de Chimie et Biologie,
Ecole Polytechnique-Université Bordeaux I-Université Bordeaux II,
Avenue Pey-Berland, 33402 Talence, France

(*Received 28 December 1999; in final form 6 March 2000; accepted 28 March 2000*)

A new homologous series of achiral banana-shaped mesogens ('D*n*') has been synthesized and studied by the classical techniques (optical microscopy, differential scanning calorimetry, X-ray diffraction, miscibility studies and electro-optic investigations). The short homologues (D6–D8) exhibit a two-dimensional phase '$B1_x$' different from a B1 phase with a rectangular lattice. The longer homologues (D9–D14) present a mesophase which displays the defects of the B7 phase of the PIMB-NO_2 compounds. Nevertheless the D9–D14 mesophase is not miscible with the B7 phase, and contrary to B7, exhibits a bistable behaviour ('ferroelectric' type) suggesting at least a B7 variant.

1. Introduction

'Banana-shaped' mesogens represent a new sub-field of thermotropic liquid crystals different from the classical calamitic systems. Indeed, their molecular structure corresponds to two rod-like mesogenic units connected to a central angular unit. As a consequence of the resulting bent shape of the molecules, which imposes peculiar packings, new mesophases, labelled 'B*n*' mesophases, are frequently observed. Molecules of this type with five, six or seven aromatic rings have been reported and recently reviewed [1], but only series of five ring mesogens have been investigated in detail. In this last case, the bent shape of these banana mesogens is due to the central 1,3 disubstituted benzene ring as shown in the following general formula:

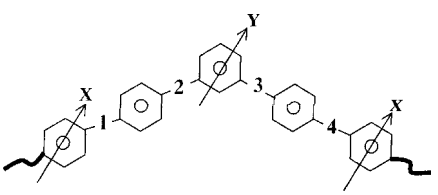

Within this formula, several elements can influence the existence and the nature of the mesophases. Nevertheless, at the moment the understanding of the relationship between chemical structure and mesomorphic properties of banana-shaped materials remains partial.

*Author for correspondence;
e-mail: achard@crpp.u-bordeaux.fr

Within the available data, it is obvious that the liquid crystalline properties of these banana mesogens are very sensitive to the nature, the position and the direction of the four connecting groups (labelled '1, 2, 3, 4'). Imino (−CH=N or −N=CH−) ester (−COO− or −OCO−), thioester (−COS− or S−CO−) or acetylenic (C≡C) groups have been used. Some sequences are mesogenic; others are not. Analysing the results of our various syntheses, mesophases appear in series where the donor or acceptor nature of the four linking groups leads to an alternate sequence of positive and negative charges on the five phenyl rings. This molecular model favours mesomorphic order [2] and for numerous examples, liquid crystalline behaviour is not detected when this condition is not satisfied. The alternate repartition of the charges on the five phenyl rings is also observed in the parent series of banana-shaped mesogens (*n*-OPIMB, with '1' = −N=CH−, '2' = −COO−, '3' = −OCO−, and '4' = −CH=N− [3, 4, 5]) where the first B phases (B1, B2, B3, B4) were discovered.

The influence of the terminal chains on the formation of the different mesophases (which is often straightforward in classical mesogens) is not completely evident. Nevertheless, in several series, two kinds of mesophase are observed depending on the length *n* of the terminal chains. For example, in the *n*-OPIMB reference series, a two dimensional B1 phase exists for short chain members ($n = 5, 6$) and a B2 smectic phase with antiferroelectric switching behaviour is observed for long homologues ($n = 7$–16). Recently, in another series ('C*n*') [6] which differs from the *n*-OPIMB compounds by the position

Liquid Crystals ISSN 0267-8292 print/ISSN 1366-5855 online © 2000 Taylor & Francis Ltd
http://www.tandf.co.uk/journals

of the linking groups (see table 1), we showed that short homologues (C5–C9) also exhibit a B1 phase, while the longer members (C10–C14) present a B2 smectic phase.

The liquid crystalline properties of the five-ring banana shaped systems appear very sensitive to an additional substituent ('*Y*') on the central ring. Thus by modifying the *n*-OPIMB structure with a $-COCH_3$, $-C_2H_5$ or $-C_6H_{13}$ group attached in position 5 or 6 of the central phenyl ring, the mesomorphic properties disappear [1]. With a chlorine atom in position 6, the B2 phase is preserved [7]. On the contrary, the introduction of a methyl or a nitro group at position 2 leads to new B mesophases (B5 when $Y = -CH_3$ [8] and B7 for $Y = -NO_2$ [9]).

The influence on the mesomorphic properties of a lateral substituent '*X*' attached at the external phenyl rings has been less studied [10–12]. Nevertheless, in series with thiocarboxylate linkages [10], one can note that the mesophase behaviour is completely changed by the introduction of a fluorine atom in the external phenyl rings. Indeed, the compounds of the series 'A*n*' (with '1' = –COS–, '2' = –OOC–, '3' = –COO–, and '4' = –SCO–) without a lateral substituent form nematic and smectic C phases, while a complex polymorphism with four smectic phases without in-plane order is observed for the corresponding 'B*n*' series with a fluorine atom attached to the external rings. In this latter case, the structure of the mesophases is not yet known.

Thus, to determine the influence of a lateral substituent *X* on the external cores, we chose to study in this paper a new series of banana-shaped mesogens ('D*n*') obtained from the basic structure of the 'C*n*' series modified by introducing a fluorine atom in position 3 on the external phenyl rings. In this manner, we hoped to keep the simplest polymorphism which would facilitate mesophase characterization.

Note finally that the assignment of the mesophases of new banana mesogens by reference to the nomenclature adopted at the Workshop on Banana-Shaped Liquid Crystals (Berlin 1997) implies hard work in characterization involving complementary techniques such as X-ray diffraction studies, microscopic observations, electro-optic measurements and phase diagram determinations. Indeed, at the present time it is difficult to establish a direct relationship between observed textures, structural peculiarities and phase assignment. We hope that the kind of work described here will contribute to defining simpler criteria for phase characterization in banana-shaped mesogens.

Table 1. Types and direction of the different linkage groups in the C*n* and D*n* series by comparison with the *n*-OPIMB reference series.

Series	1	2	3	4	*X*
n-OPIMB	–N=CH–	–COO–	–OOC–	–CH=N–	H
C*n*	–COO–	–N=CH–	–CH=N–	–OOC–	H
D*n*	–COO–	–N=CH–	–CH=N–	–OOC–	F

2. Materials

These new symmetric banana-shaped molecules (Series D) correspond to the general formula:

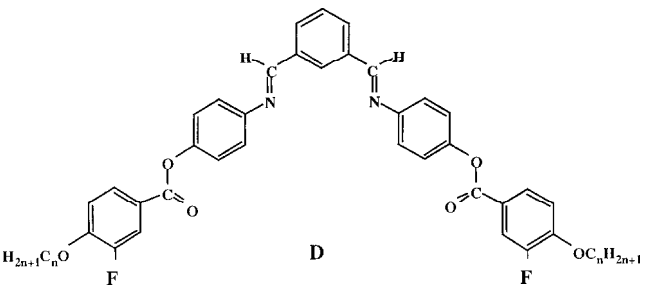

The materials are labelled D*n*, where *n* is the number of carbon atoms in the terminal alkoxy chain and $n = 6–14$. In these molecules the azomethine groups are linked to the 1,3 positions of the central phenyl ring and the ester groups are placed between the two external phenyl rings and thus they differ from the *n*-OPIMB reference series [3–5] by the position of the connecting groups (see table 1). A fluorine atom is attached in position 3 on the external phenyl rings.

3. Synthesis

The members of the 1,3-bis[4-(3-fluoro-4-*n*-alkoxybenzoyloxy)phenyliminomethyl] phenylene (series D*n*) were synthesized according to the scheme in figure 1.

The 3-fluoro-4-alkoxybenzoic acids (compounds **2**) used in the process were prepared according to the method [13] summarized in figure 2.

Isophthalaldehyde (0.1 mol) and 4-aminophenol (0.2 mol) were dissolved in boiling absolute ethanol in the presence of a few drops of acetic acid. The solution was heated at reflux for 3 h. This condensation led to the 1,3-bis[4-hydroxypheny liminomethyl] phenylene (**1**), which was recrystallized three times from a heptane/ethanol mixture. To obtain the members of the series D*n*, the appropriate 3-fluoro-4-*n*-alkoxybenzoic acid (2 mmol) and compound **1** (1 mmol) were interacted in dichloromethane with dicyclohexylcarbodiimide (2.2 mmol) and 4-dimethylaminopyridine as catalyst. The mixtures were stirred at room temperature for about 24 h. The products were recrystallized three times from ethanol/toluene and twice from toluene/heptane; yields 30–50%. The following analytical data are given as being representative for the D14 homologue. ^{1}H NMR (200 MHz, $CDCl_3$) δ (ppm): 8.6 (2H, s, CH=N), 8.4 (1H,

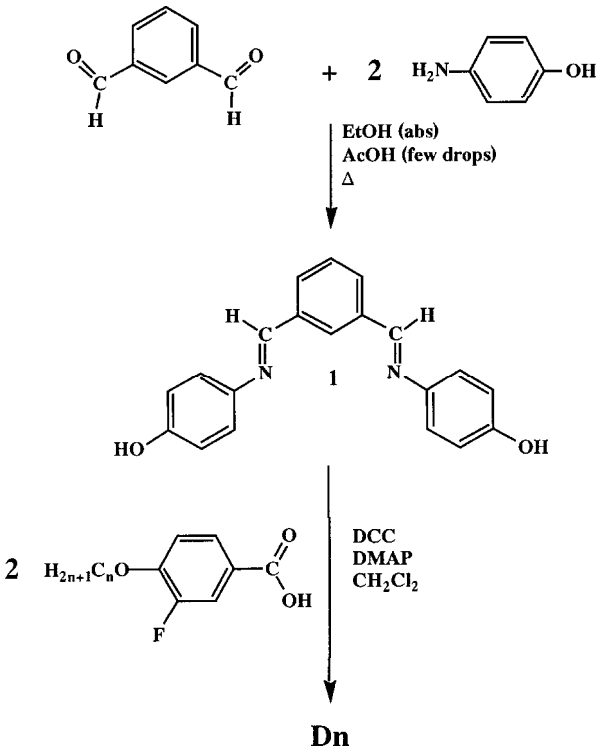

Figure 1. Synthesis of the D*n* mesogens.

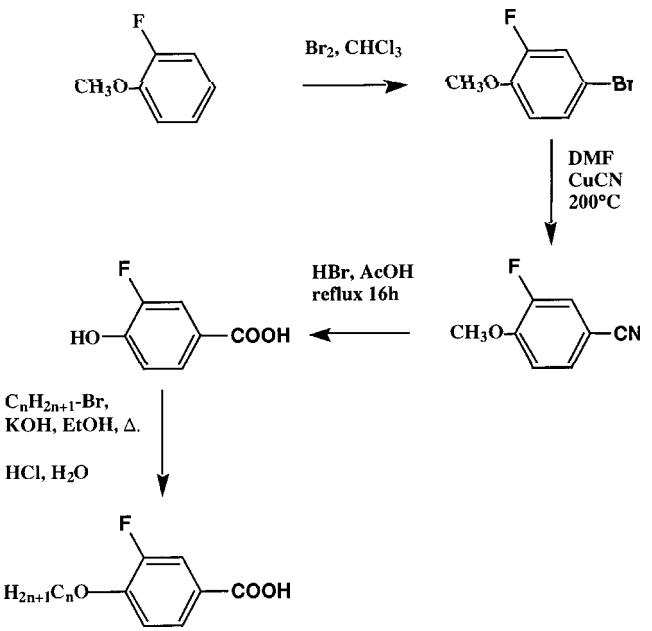

Figure 2. Synthesis of 3-fluoro-4-alkoxybenzoic acids.

s, Ar–H), 7.88–8.05 (6H, m, Ar–H), 7.6 (1H, t, Ar–H), 7.22–7.34 (8H, m, Ar–H), 7.1 (2H, t, Ar–H), 4.1 (4H, t, O–$\underline{CH_2}$), 1.9 (4H, t, O–CH_2–$\underline{CH_2}$), 1.25–1.5 (44H, m, CH_2), 0.85–0.9 (6H, m, CH_3).

4. Experimental methods

Thermal behaviour was investigated using a Perkin-Elmer DSC7 differential calorimeter. The optical textures of the mesophases were observed using a polarizing microscope (Leitz Diavert) equipped with a hot stage (FP-82HT) and an automatic temperature controller (Mettler FP-90). Samples were observed on regular slide glass without any surface treatment.

X-ray diffraction experiments were carried using an 18 kW rotating anode X-ray source (Rigaku-200) with the use of a Ge(1 1 1) crystal as monochromator. The scattered radiation was collected on a two-dimensional detector (Imaging Plate system from Mar Research, Hamburg). The samples were placed in an oven, providing a temperature control of 0.1 K.

Electro-optical properties were studied using commercial cells (from E.H.C., Japan) with rubbed polyimide layers (but the surface treatment is not effective for making uniformly oriented cells). Switching current was observed by applying a voltage-wave using a function synthesizer (HP 331 20A) and a high power amplifier (Krohn-Hite).

5. Experimental results

The transition temperatures and associated enthalpies are listed in table 2. As expected, only one mesophase (phase 1 or phase 2) was observed for each compound of series D.

Table 2. Transition temperatures (°C) and enthalpies (italics, ΔH kJ mol^{-1}) as a function of the number of carbon atoms in the terminal tails (from DSC runs, increasing temperature, rate 5°C min^{-1}). The distinction between the two mesophases results from microscopic observations and X-ray analysis.

n	Cr		Phase 1		Phase 2		I
6	•	107.3 *32.3*	•	165.2 *22.3*	—		•
7	•	109.5 *34*	•	163.8 *23*	—		•
8	•	111.8 *33.4*	•	162.0 *23.4*	—		•
9	•	112.8 *32.9*			•	160.3 *22.9*	•
10	•	111.5 *33.9*	—		•	158.9 *22.7*	•
11	•	111.7 *34.8*	—		•	158.3 *23.5*	•
12	•	111 *31.7*	—		•	157 *22.7*	•
13	•	110.7 *48*	—		•	156.6 *23*	•
14	•	110 *50*	—		•	155.3 *22.7*	•

The dependence of the melting and clearing points on the length of the terminal chains is compared in figure 3 for the C*n* and D*n* series: the stable temperature range of the mesophase widens on introducing fluorine in the external phenyl rings due to the usual decrease of the melting point and the unusual enhancement observed for the clearing temperatures. The stabilization of the mesophase illustrates the first influence of fluorine substituents on the external rings of such systems. As for the C*n* series, textural analysis of the D*n* series clearly suggests two kinds of mesophase, one for the short homologues (D6–D8) and another for long homologues (D9–D14).

5.1. *Short homologues (D6–D8)*

5.1.1. *Microscopic observations*

On cooling the isotropic state, the mesophase of the short chain members of the D series grows as circular domains which coalesce (see figure 4).

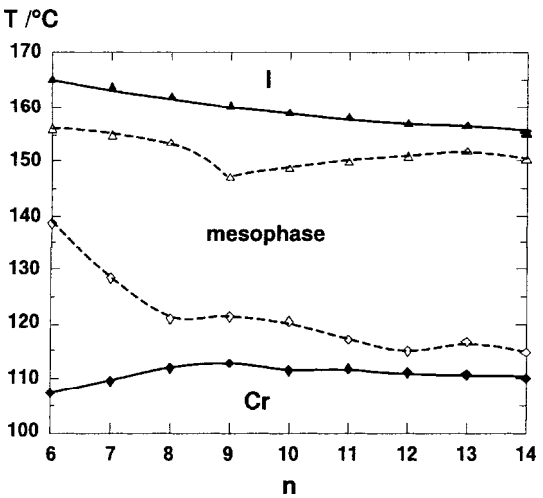

Figure 3. Comparison of the melting and clearing temperatures of the C*n* (dotted lines) and D*n* (full lines) series.

5.1.2. *X-ray analysis*

The X-ray patterns of the D6–D8 homologues exhibit diffuse scattering at wide angles, showing the absence of in-plane order within the layers. The small angle region is characterized by four reflections (e.g. for D7: two intense reflections at $q = 0.160$ and $0.307\,\text{Å}^{-1}$ which cannot be assigned to the first and second layer reflections, and two weaker ones at $q = 0.088$ and $0.205\,\text{Å}^{-1}$). As deduced from X-ray analysis of imperfectly oriented samples, the Bx phase of the D7 compound is a two dimensional phase. Nevertheless, it seems structurally different from the B1 phase of the isomeric non-fluorinated C7 [6] which is characterized by only two reflections located at 0.235 and $0.302\,\text{Å}^{-1}$ (see figure 5). To confirm the difference between the B1 and Bx phases, we have completed the comparison of the mesomorphic behaviour of the two compounds with a study of their miscibility phase diagram.

5.1.3. *Miscibility studies with a B1 phase*

Mixtures at given composition have been prepared and analysed using the three classical techniques of investigation. The resulting diagram is shown in figure 6. The clearing temperature varies smoothly from C7 (left) to D7 (right). The melting temperatures also show a remarkable regularity with no marked eutectic. These features would suggest an easy mixing of these chemically similar compounds, whatever the physical state. However, in the mesomorphic range, the connection between the B1 phase of C7 and the Bx phase of D7 is not straightforward since a strong non-ideal behaviour in the form of an injected mesophase is observed. Below 140°C, this bell-shaped domain separates the B1 and Bx phases and extends over a large range of composition†. Above

†There is no doubt about the monophasic homogeneous character of this domain from thermal and structural analysis, although the bell shape could also suggest a miscibility gap. X-ray patterns recorded within this domain exhibit a complex profile different from both the B1 and the Bx phases with new reflections characteristic of this third mesophase.

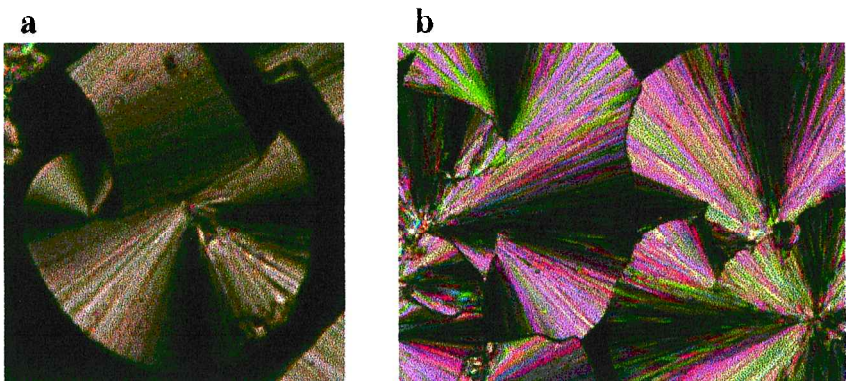

Figure 4. Growth of circular domains on cooling from the isotropic phase: (*a*) compound D7, $T = 159$°C; (*b*) compound D8, $T = 157$°C.

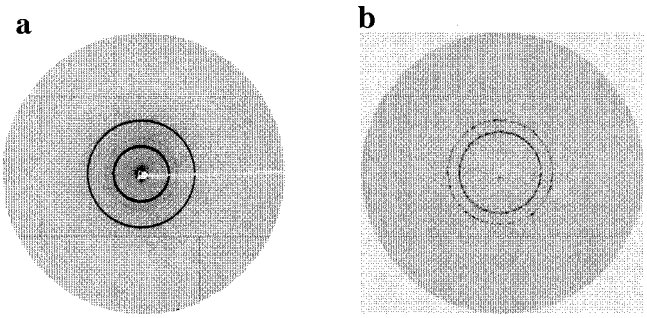

Figure 5. Non-oriented X-ray patterns (*a*) of the D7 homologues and (*b*) of compound C7 in the B1 phase for comparison ($q = 0.235$ Å^{-1} and $q = 0.302$ Å^{-1}).

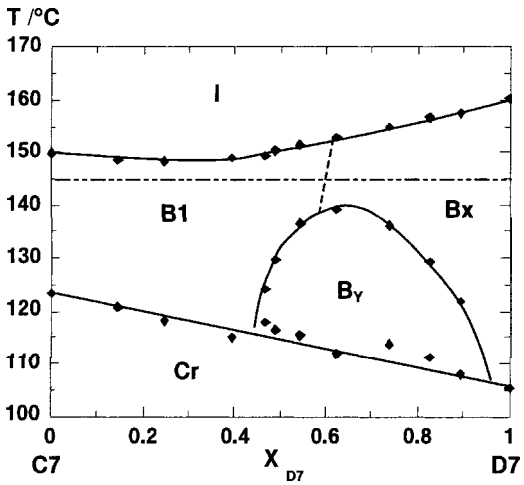

Figure 6. Binary phase diagram between compound C7 and compound D7. The horizontal dotted line indicates the path followed for the structural data of figure 8.

140°C, in a contact preparation (figure 7), the contact zone remains between the B1 and Bx textures. At this stage the connection between B1 and Bx had not been solved. To discuss this point we present in figure 8 the structural analysis conducted along an isothermal path at 145°C: the two parameters of the B1 phase are observed up to the mixture next to the maximum of the injected phase on the side rich in C7 ($x_{D7} \leqslant 0.55$). Beyond this composition the four reflections of the Bx phase remain distinct even though there appears a rapid evolution of the parameters in the mixture closest to the maximum ($x_{D7} = 0.63$). The conclusion is that a phase transition necessarily exists between ($0.55 < x_{D7} < 0.63$), the phase line of which is consequently very steep and very difficult to detect (dotted line in figure 6). This occurrence of almost vertical lines of phase equilibrium separating B phases has been previously noticed in other phase diagrams [6, 14]. Thus the two dimensional Bx mesophase of the short D*n* homologues is distinct from a two dimensional B1 phase with a rectangular lattice. The evolution of the structural data in the C7–D7 binary

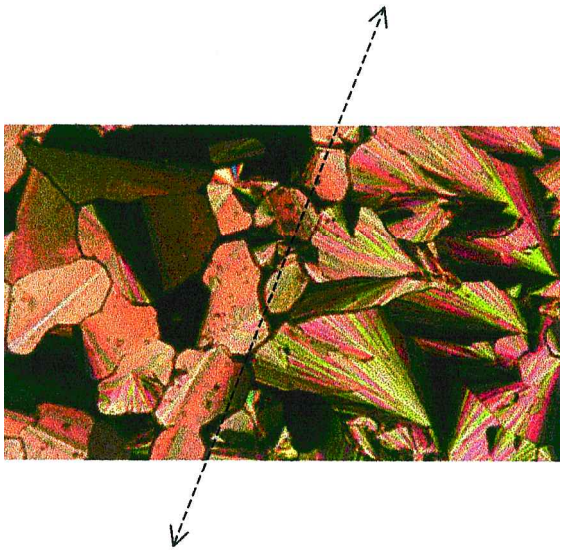

Figure 7. Microphotograph of a contact preparation between compound C7 in the B1 phase (left) and compound D7 (right) at 45°C (the arrow indicates the contact line).

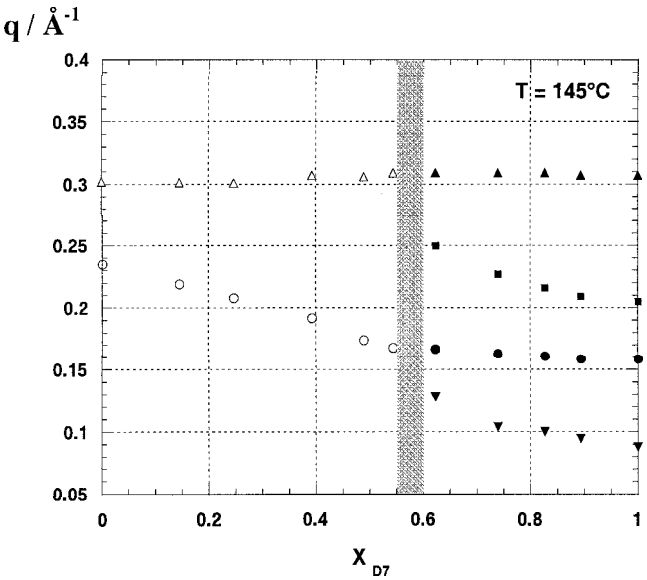

Figure 8. Evolution of the structural data in the C7–D7 binary diagram at constant temperature $T = 145$°C (C7: $q = 0.235$ and 0.302 Å^{-1}; D7: $q = 0.088$, 0.160, 0.205 and 0.307 Å^{-1}).

diagram suggests a different lattice, which is progressively distorted to join the parameters of the rectangular lattice of the B1 phase. In these conditions, as for columnar phases, we suggest adding an index to the B1 label: $B1_r$ for a rectangular lattice and $B1_x$ for this new phase, where 'x' corresponds to the lattice type which cannot be more precisely defined without oriented samples.

5.2. *Long homologues (D9–D14)*

For long chain members, the phase behaviour is completely different.

5.2.1. *Microscopic observations*

On slow cooling from the isotropic liquid, a large variety of textures arises for long homologues. These texture variants frequently occur at different places within the same sample preparation. Some representative examples are given in figure 9. The mesophase can form radial domains and elongated germs or nuclei growing into shapes such as banana-tree leaves (*a*). Different kinds of spiral germ are observed indicating a helicoidal structure (*b*). Ribbons with equally spaced lines (*c*), and myelinic textures (*d*) frequently occur. The observation of free droplets reveals fan-shaped textures with regularly spaced stripes (*e*). Sometimes, very beautiful two-dimensional periodic patterns are visible (*f*).

Many of the texture variants observed for the D9–D14 compounds remind one of the texture of the B7 mesophase evidenced in the *n*OPIMB reference series with the central core substituted in the 2-position by a nitro group (*n*OPIMB-NO_2 for short) [9].

5.2.2. *X-ray analysis*

In the X-ray patterns a diffuse scattering in the wide angle region indicates a liquid-like order within the layers. However, in the small angle regions, the observed reflections (figure 10 and table 3) exclude a simple layer structure. Indeed, in addition to a very intense peak at a wave vector q_2 with two or three harmonics, two additional weaker reflections are observed: one is at very small angle (wave vector q_1) and another at larger angle (wave vector q_3). These reflections cannot be assigned without perfectly oriented samples, but the partial orientation obtained does show that the q_1 and q_2 wave vectors point in different directions. The D9–D14 mesophase has probably a two-dimensional structure, complicated by a helicoidal superstructure as shown by the spiral defects observed in the microscopic textures, figure 9 (*b*).

In figure 11, the evolution of the X-ray data throughout the D*n* series is reported. The linear evolution of the wave vector corresponding to the more intense reflection within the two different two-dimensional structures is worth noting: the $B1_x$ phase for short chain compounds and the mesophase of the long homologues.

The powder patterns of the D9–D14 compounds remind one of the patterns of the B7 mesophase of the *n*OPIMB-NO_2 series. Indeed, in the B7 phase of the *n*OPIMB-NO_2 homologues, four main reflections are also observed at low angles (table 4) with their harmonics: one intense reflection could correspond to the main reflection 'q_2' in the D*n* series and the reflection at very small angles to 'q_1' in the D*n* series. The other peaks may correspond to the weaker reflections observed in the D*n* series.

Thus the microscopic textures as well as the X-ray patterns of the D9–D14 mesophase support the hypothesis of a B7 mesophase. To confirm this assignment, we now study the binary phase diagram between the 14-OPIMB-NO_2 and the D14 compounds.

5.2.3. *Miscibility studies with the B7 phase of the n-OPIMB-NO_2 compounds*

The 14-OPIMB-NO_2/D14 binary diagram is reported in figure 12. It results from complementary techniques: microscopic observations, DSC measurements and X-ray analysis of mixtures at given concentration.

This diagram presents three main characteristics: (i) very large isotropic liquid/mesophase biphasic domains easily seen under the microscope, (ii) a non-linear evolution of the clarification temperature with a deep minimum indicating the low compatibility of the two compounds, which is confirmed by the (iii) appearance in the mesomorphic range of a wide domain of phase

Table 3. Characteristic wave vectors q ($q = 2\pi/d$) corresponding to the main reflections observed in the long chain members of the D*n* series (the corresponding distances in real space, in Å, are indicated between brackets). Other reflections exist but they are too weak to be analysed.

n	q_1/Å^{-1}	q_2/Å^{-1} highest intensity reflection	q_3/Å^{-1}	$q_4 = 2q_2$/Å^{-1}
9	0.048 (130)	0.152 (41.3)	0.294 (21.4)	0.305
10	0.040 (157)	0.146 (43.0)	0.286 (21.9)	0.300
11	0.039 (161)	0.144 (43.6)	0.276 (22.7)	0.288
12	0.041 (153)	0.139 (45.2)	0.268 (23.4)	0.280
13	0.052 (121)	0.132 (47.6)	0.264 (23.8)	0.265
14	0.052 (121)	0.128 (49.1)	0.256 (24.5)	0.257

Table 4. Characteristic wave vectors q ($q = 2\pi/d$) corresponding to the main reflections at low angles observed in the B7 mesophase of the *n*OPIMB-NO_2 series (the corresponding distances in real space, in Å, are indicated between brackets). In addition, several harmonics are observed.

n	/Å^{-1}	/Å^{-1}	highest intensity reflection/Å^{-1}	/Å^{-1}
8	0.059 (106)	0.121 (51.9)	0.177 (35.5)	0.204 (30.8)
9	0.056 (112)	0.118 (53.2)	0.169 (37.1)	0.193 (32.5)
10	0.053 (118)	0.111 (56.6)	0.162 (38.8)	0.183 (34.3)
11	0.051 (123)	0.107 (58.7)	0.156 (40.2)	0.175 (38.9)
12	0.044 (143)	0.100 (62.8)	0.151 (41.6)	0.170 (36.9)
14	0.039 (161)	0.079 (79.5)	0.139 (45.2)	

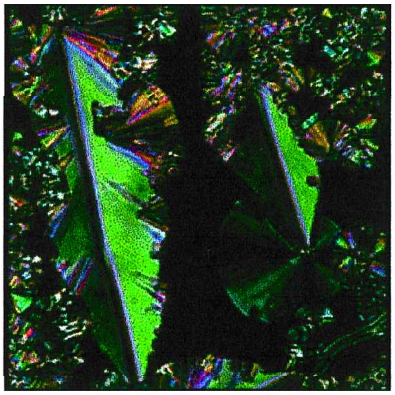

(*a*)

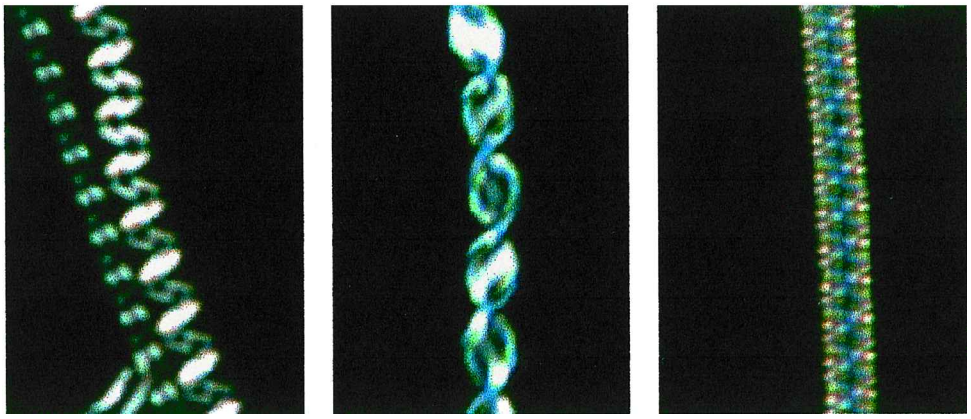

(*b*)

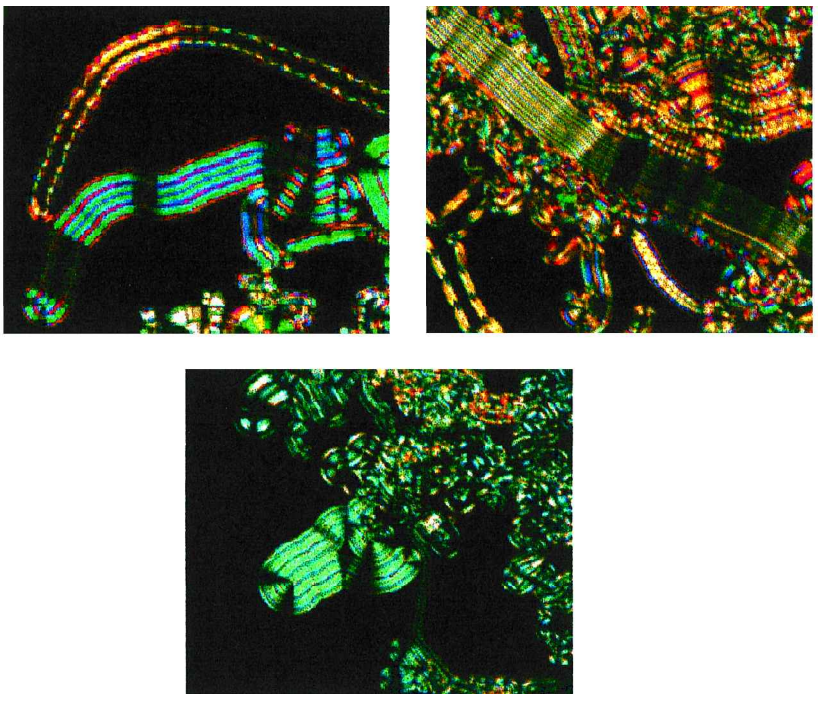

(*c*)

Figure 9. (*a*) Growth of circular domains and of elongated germs or nuclei giving domains like banana-tree leaves (D11 at 157.5°C); (*b*) different spiral nuclei (D14 at 153°C); (*c*) growth of ribbons with regularly spaced lines (D9 at 157.5°C); (*Continued*) (*d*) myelinic texture (D13 at 154.5°C); (*e*) regularly spaced lines observed on a free droplet (D10 at 156.5°C); (*f*) examples of two-dimensional periodic patterns (D14 at 153°C).

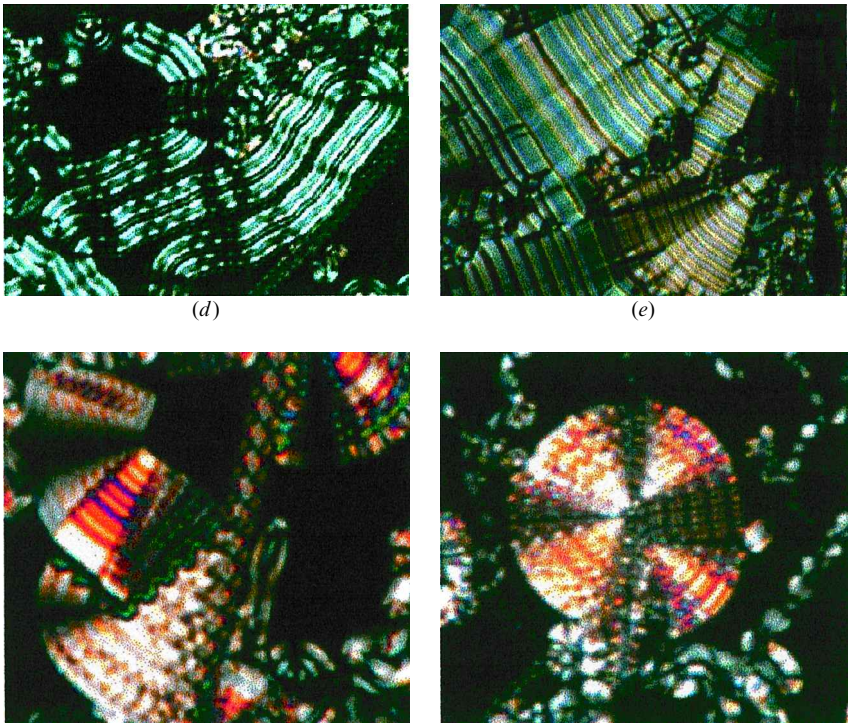

(*d*) (*e*)

(*f*) (*g*)

Figure 9. (*continued*).

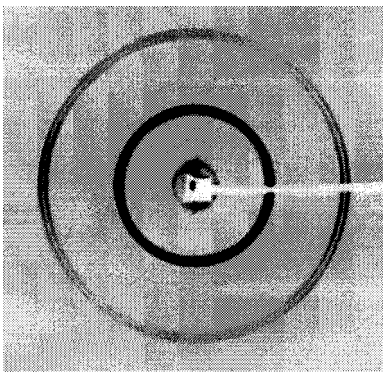

Figure 10. Partially oriented pattern of compound D10 at 150°C. The two wave vectors q_1 (0.040 Å^{-1}) and q_2 (0.146 Å^{-1}) point in different directions.

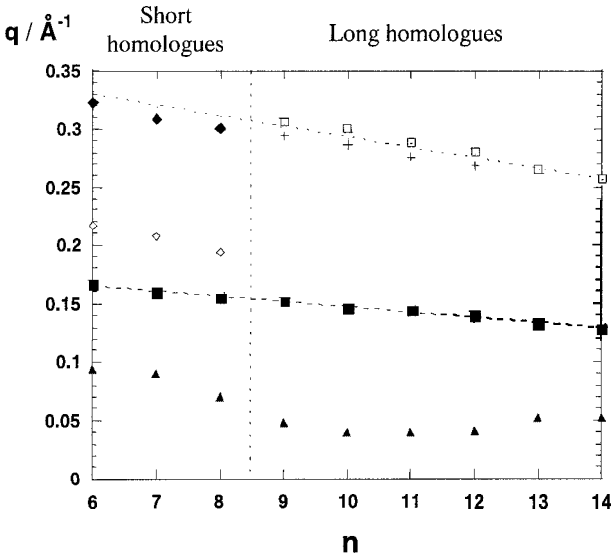

Figure 11. Evolution of the main reflections in the D*n* series: a clear distinction can be made between short chain homologues and longer ones.

separation. The B7 and D14 mesophases are thus separated by a biphasic domain which extends over a large concentration range. Therefore, the bidimensional structures and/or the helicoidal superstuctures of the B7 phase of the 14-OPIMB-NO_2 and of the D14 mesophase are incompatible. Of course this miscibility gap does not exclude the possibility that both phases belong to the same type. Nevertheless, one must note that the phase diagram between two *n*-OPIMB-NO_2 homologues ($n = 8$ and $n = 12$) shows a complete miscibility of the two B7 mesophases, despite rather different parameters as shown in table 4; also a linear evolution of the temperatures and of the structural data is observed [15].

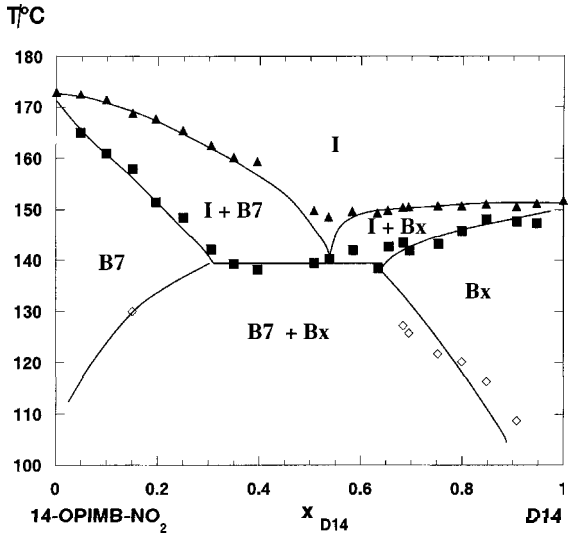

Figure 12. Binary phase diagram between 14-OPIMB-NO_2 which presents a B7 mesophase and compound D14. A large biphasic domain separates the B7 and the Bx mesophase of D14.

5.2.4. *Electro-optic studies*

Contrary to the short chain members and the B7 mesophase of the *n*-OPIMB-NO_2 series [9], D9–D14 mesophases show an electro-optical switching. As an example, in figure 13, the switching behaviour of the D10 compound in the mesophase under an electric field is shown to be of the bistable kind (i.e. 'ferroelectric' type) with a rather high threshold ($\approx 10\ V\ \mu m^{-1}$). The switching behaviour is identical for all the long chain members, except for the threshold which slightly increases when the chain length decreases. The polarization value lies between 300 and 380 $nC\,cm^{-2}$ for the D9–D14 homologues, the typical response time is 100 µs and the threshold 10 $V\ \mu m^{-1}$. No significant variation is observed as a function of temperature in the mesophases.

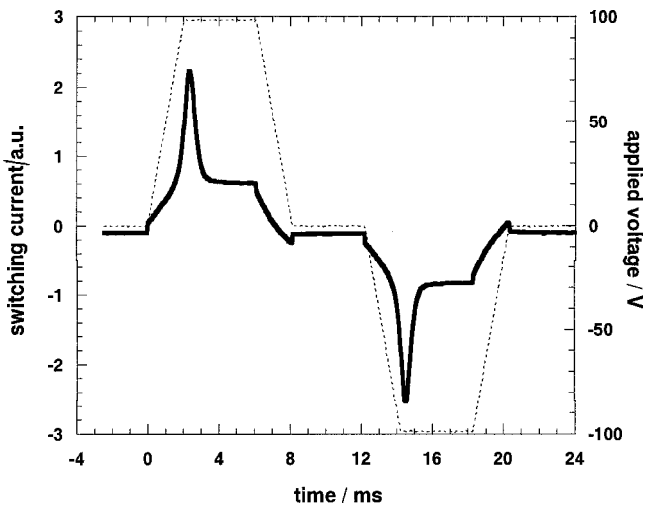

Figure 13. Switching current response in the mesophase of compound D10 obtained by applying a modified triangular voltage (± 100 V), sample thickness 5.4 µm, $T = 120°C$.

This observation of a bistable switching in this banana phase is different from the transient phenomenon in freshly prepared samples already reported in [6, 7] or as Niori *et al.* probably first observed in a B2 mesophase [3]. Up to now, most of the switching banana phases, B2 [6, 7, 16], B5 [8] and the 'B7' mesophase of the fluorine or sulfur containing derivatives 10-OPIMB(F) [11] and PSPIMB [12]† show an antiferroelectric type switching, as soon as the applied voltage is higher than a switching threshold. Only one example of bistable switching has been recently reported in banana compounds [17].

We have used a modified triangular voltage with plateaux at $-V$, 0 and $+V$, respectively, in order to let the switching be complete at $+/-\ V$ even in the case of a slow response time and to check that the polarized state remains stable when the applied voltage vanishes. This kind of voltage waveform with multiple steps allows for a deconvolution of polarization reversal curves made of several mixed humps. In fact, one can establish a clear difference between bistable phases ('ferroelectric' type) where the state reached at $+V$ (or alternatively $-V$) is conserved when the voltage is switched off and monostable phases ('antiferroelectric' type) where one always returns to the same state at zero voltage. In the first case there is a polarization hump at each reversal between the + P and the − P states, while in the second one, each creation or annihilation of the polarization leads to a separate hump.

In the case of the B7 phase of the *n*-OPIMB-NO_2 compounds, no switching is observed under an electric field [9]; this we have checked for 11-OPIMB-NO_2 up to $50\ V\ \mu m^{-1}$ with the same experimental set-up. Twinkling areas corresponding to electro-hydrodynamical instabilities are observed at lower field in *n*-OPIMB-NO_2 and the D*n* series, but they are clearly not at the origin of the polarization hump observed in the D9–D14 compounds. Therefore if the B7 and D9–D14 mesophases belong to the same type, one has to assume that the switching threshold is never reached up to $50\ V\ \mu m^{-1}$ for the *n*-OPIMB-NO_2 materials.

6. Discussion

At this stage, the problem of the nomenclature of the banana mesophases is raised again. Despite similar textures and rather comparable powder patterns, an

† Note that our X-ray experiments show a simple layered structure for the 'B7' phase of 12-SPIMB and for 14-OPIMB(F) which is incompatible with the complex pattern of the B7 phase of the PIMB-NO_2 derivatives.

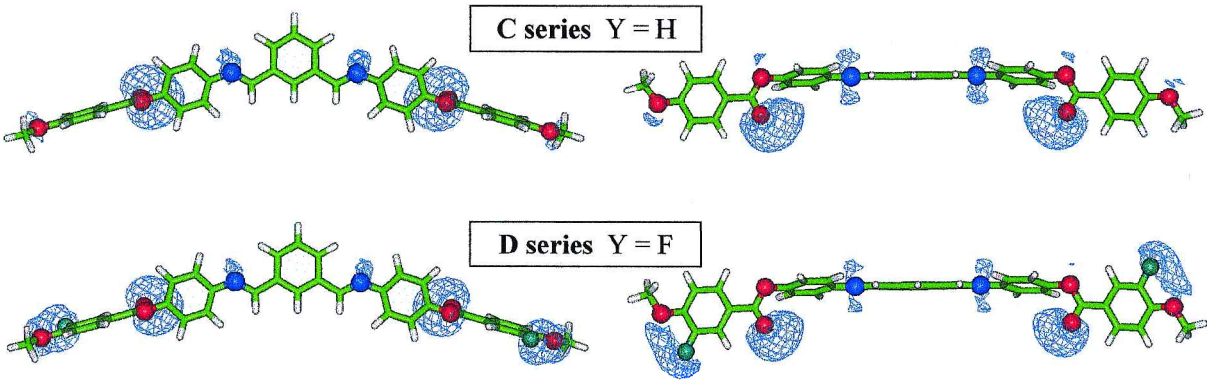

Figure 14. Influence of the presence of a fluorine atom on the external rings on the repartition of the negative potential (in blue) along the molecules. The example of the *n*-OPIMB-NO_2 molecules which form the B7 mesophase is given for comparison (same energy scale).

uninterrupted miscibility domain between the B7 phase of *n*-OPIMN-NO_2 and the mesophase observed for the D9–D14 compounds is not found. The clear difference in the electro-optical responses suggests a new phase type, at least a B7 variant for the D9–D14 mesophase. Nevertheless, to avoid additional complication of an already complex phase nomenclature situation in banana mesophases, we suggest using the '$B7_{bis}$' label for long chain members of the D series, until X-ray data on oriented samples can be obtained.

This work clearly underlines the difficulties encountered in characterizing the mesophases of banana-shaped mesogens, difficulties which are due to the factors detailed below.

The microscopic textures are not characteristic of one mesophase. The most spectacular example concerns the 'B7 defects' (such as spirals, ribbons ...) of the PIMB-NO_2 compounds which are observed in several other cases; either in a mesophase with multiple scattering structures, as observed for the D*n* compounds or in MHOBOW [18] (both of which exhibit a bistable behaviour), or in a mesophase exhibiting a simple layered structure like 10-OPIMB(F) [11] and PSPIMB [12], or in the new banana-shaped mesogens we have synthesized [19].

Except for smectic mesophases, such as B2 or B5, perfectly oriented sample are hard to obtain. In these conditions, the nomenclature used, which is not based on structural data, appears insufficient to describe the B mesophases and to correlate an unknown mesophase with those previously labelled.

Miscibility studies are also laborious. Indeed, the banana-shaped mesogens form 'fluid' mesophases in the sense that no positional order is detected within the layers. Nevertheless due to the bent shape of the molecules, the corresponding packings in the mesophases are rather rigid as indicated by the strong isotropic–mesophase transition enthalpies. In such cases, sufficiently different structural parameters may lead to a gap of miscibility, even if the mesophases belong to the same type.

Finally, comprehension of the relationship between chemical structure and mesomorphic behaviour for banana mesogens is still at the initial stages. Many parameters (the length of the terminal chain, the position and the orientation of the linking groups and the substituents on the different phenyl rings) influence the mesomorphic properties, sometimes in a dramatic manner. The example shown in this paper, the introduction of a lateral fluorine substituent in position 3 on the terminal phenyl rings (which seems to be a minor modification!) leads to a drastic change of the mesomorphic behaviour (from a smectic B2 to a '$B7_{bis}$' mesophase). Other variants of the D series give evidence of a subtle relationship between the molecular structure and the mesomorphic properties: a chlorine atom in position 3 or two fluorine atoms in positions 2 and 3 give the same '$B7_{bis}$' mesophase, while a lateral fluorine substituent in position 2 reveals a B2 phase. It is clear that in bent mesogens, steric hindrance as well as the electrostatic repartition will strongly influence the presence and the nature of the mesophases. Figure 14 shows the electrostatic potential† of series C and D. It is clear that the presence of a fluorine in position 3 in series D slightly reduces the negative electrostatic potential around the Schiffs base group (-24 kcal mol^{-1} in D versus -26 kcal mol^{-1} in C) and around the ester group (-49 kcal mol^{-1} in D versus -53 kcal mol^{-1} in C) and at the same time strongly reinforces the potential between

† The electrostatic potential is calculated by the VSS method on lowest energy conformers found after Monte-Carlo space conformation studies. Charge calculations were performed by using the MOPAC semi-empirical package with the MNDO method and potential contours are drawn at -20 kcal mol^{-1} in blue.

the fluorine and the methoxy group (-31 kcal mol^{-1} in D versus -23 kcal mol^{-1} in C). That is to say, the presence of the fluorine atom in D strongly modifies the repartition of the electrostatic potentials in the surrounding space from $-26/-53/-23$ kcal mol^{-1} in series C to $-23/-49/-31$ kcal mol^{-1} in series D, with a concomitant lowering of the central space and a strengthening of the outer space, which can lead to a large modification of the mesomorphic properties.

References

[1] Pelzl, G., Diele, S., and Weissflog, W., 1999, *Adv. Mater.*, **11**, 9 and references therein.

[2] Nguyen, H. T., Rouillon, J. C., Marcerou, J. P., and Barois, P., 1999, in Proceedings of the Liquid Crystal Conference, Strasbourg (D2-O3).

[3] Niori, T., Sekine, T., Watanabe, J., Furukawa, T., and Takezoe, H., 1996, *J. Mater. Chem.*, **6**, 1231.

[4] Sekine, T., Niori, T., Sone, M., Watanabe, J., Choi, S. W., Takanishi, Y., and Takezoe, H., 1997, *Jpn. J. appl. Phys.*, **36**, 6455.

[5] Heppke, G., Krüercke, D., Löhning, C., Lötzsch, D., Rauch, S., and Sharma, N. K., 1997, Freiburger Arbeitstagung Flüssigue Kristalle (poster P70).

[6] Bedel, J. P., Rouillon, J. C., Marcerou, J. P., Laguerre, M., Achard, M. F., and Nguyen, H. T., 2000, *Liq. Cryst.*, **27**, 103.

[7] Pelzl, G., Diele, S., Grande, S., Jakli, A., Lischka, C., Kresse, H., Schmalfuss, H., Wirth, I., and Weissflog, W., 1999, *Liq. Cryst.*, **26**, 401.

[8] Diele, S., Grande, H., Kruth, H., Lischka, C., Pelzl, G., Weissflog, W., and Wirth, I., 1998, *Ferroelectrics*, **212**, 169.

[9] Pelzl, G., Diele, S., Jakli, A., Lischka, C., Wirth, I., and Weissflog, W., 1999, *Liq. Cryst.*, **26**, 135.

[10] Nguyen, H. T., Rouillon, J. C., Marcerou, J. P., Bedel, J. P., Barois, P., and Sarmento, S., 1999, *Mol. Cryst. liq. Cryst.*, **328**, 177.

[11] Lee, C. K., and Chien, L. C., 1999, in Proceedings of 7th International Conference on Ferroelectric Liquid Crystals, Darmstadt.

[12] Heppke, G., Parghi, D. D., and Sawade, H., 1999, in Proceedings of International Conference on Ferroelectric Liquid Crystals, Darmstadt.

[13] Nabor, M. F., Nguyen, H. T., Destrade, C., Marcerou, J. P., and Twieg, R. J., 1991, *Liq. Cryst.*, **10**, 785.

[14] Bedel, J. P. Nguyen, H. T., Rouillon, J. C., Marcerou, J. P., Sigaud, G., and Barois, P., 1999, *Mol. Cryst. liq. Cryst.*, **332**, 163.

[15] Bedel, J. P. (to be published).

[16] Link, D. R., Natale, G., Shao, R., Maclennan, J. E., Clark, N. A., Körblova, E., and Walba, D. M., 1997, *Science*, **278**, 1924.

[17] Walba, D. M., Körblov, A. E., Shao, R., Maclennan, J. E., Link, D. R., and Clark, N. A., 1999, abstract in 7th International Conference on Ferroelectric Liquid Crystals, Darmstadt.

[18] Link, D. R., Chattham, N., Clark, N., Körblova, E., and Walba, D., 1999, abstract in 7th International Conference on Ferroelectric Liquid Crystals, Darmstadt.

[19] Bedel, J. P. (to be published).